Metallography, Microstructure, and Analysis (2024) 13:452–461
https://doi.org/10.1007/s13632-024-01067-0

ORIGINAL RESEARCH ARTICLE

Metallographic and Extraction Replica Methods for Characterization of Tungsten Heavy Alloy: H13 Clads

Jerry Kovacich[1] · Dennis Harwig[1] · Andreas Endemann[2]

Received: 10 October 2023 / Revised: 27 January 2024 / Accepted: 11 February 2024 / Published online: 15 May 2024

Abstract

Tungsten heavy alloys are used in demanding high pressure die casting applications due to their high temperature strength, high thermal conductivity, and low thermal expansion. High cost limits applications to small sintered die inserts and manual gas tungsten arc weld repairs. A new tungsten heavy alloy consumable, Anviloy wire, was developed for automated cladding of hot work tool steel dies. Literature regarding characterization of tungsten heavy alloy die steel clads was lacking. Understanding base metal dilution effect on clad microstructure is critical but required new sample preparation methods. An Anviloy wire-H13 clad was made using hot wire gas tungsten arc cladding and analyzed with metallography. Samples were found to have grain boundary M_6C carbide phase as-welded with the help of an alkaline sodium picrate etchant. An isothermally aged arc crucible melted sample of the same composition was characterized using metallography, scanning electron microscopy, and transmission electron diffraction. The clad representative arc crucible melted sample was subjected to isothermal aging at 725°C for 100 hours. Isothermal aging resulted in precipitation of a high volume fraction of intermetallic platelets. Using a new carbon extraction replica sample preparation method involving two chemical polishing steps, transmission electron diffraction of precipitates indicated they were mu phase intermetallic.

Keywords Welding · Refractory metals · Thermal stability · Metallography · Cladding

Introduction

Tungsten heavy alloys are used in defense applications for armor and kinetic penetrators, in high pressure die casting as mold materials, and as weights in aerospace and commercial applications [1–3]. They have high density based on their high volume fraction of dense alpha BCC tungsten phase. The tungsten phase imparts also provides good high temperature strength, low thermal expansion, and high thermal conductivity. These alloys differ from pure tungsten alloys in that individual tungsten particles are embedded in a lower melting point matrix phase. The matrix phase in tungsten heavy alloys melts and wets tungsten particles to infiltrate and fill voids between them, forming a densified structure composed of two metallic phases [2, 4, 5]. The most widely used tungsten heavy alloys are the W-Ni-Fe type [2]. An interesting attribute of the W/Ni/Fe ternary system is their tendency to solidify without forming intermetallics [6–9]. This characteristic allows enables liquid phase sintering of tungsten rich alloys that exhibit good properties for the above applications. The W-Ni-Fe ternary system has been evaluated by numerous researchers over the last century [6–8, 10–15]. Winkler and Vogel produced the first ternary diagram, showing that W-Ni-Fe alloys can solidify as metallic alpha BCC tungsten and gamma FCC phases over a wide compositional range [6].

Infiltration of tungsten grains by the lower melting point matrix phase allows for much lower processing temperatures compared to pure tungsten alloys while still providing similar strength, low thermal expansion, and thermal conductivity [2, 3]. For these alloys, the FCC matrix phase improves low and intermediate temperature ductility and fracture toughness [9]. The matrix phase improves these properties by preventing gross cracking of tungsten phase, which has a high ductile to brittle transition temperature between 100 and 450 °C [16, 17].

For die casting applications, the Anviloy® series of alloys have been used since the 1970's for the most severe thermal

✉ Jerry Kovacich
kovacich.2@osu.edu

[1] The Ohio State University, Columbus, OH, USA

[2] Weldstone Gmbh, Burbach, Germany

fatigue die conditions [18]. These liquid phase sintered tungsten heavy alloys are limited to the most aggressive die environments due to high cost. Weld consumables are available but were historically limited to rod form, making cladding / hardfacing of tool steel dies inefficient. Recently, an Anviloy wire consumable was developed for use in automated welding processes that can support die cladding, repair and additive manufacturing of features [19]. Research was needed to develop process—microstructure—performance relationships for Anviloy cladding on H13 tool steel. Methods to characterize intermetallics which precipitate on thermal exposure in tungsten heavy alloy—tool steel clads are lacking in literature. This study characterized an Anviloy wire-H13 clad as-deposited in addition to an arc crucible melted sample with the same composition aged at 725 °C for 100h.

Thermal exposure experiments were designed to represent surface microstructure aging in die casting dies. In die casting, temperature drops rapidly from a maximum at die surface. A large thermal gradient exists between the surface and the bulk die's thermal mass. Temperature gradients are heightened by the presence of coolant lines provide die cooling to reduce casting cycle time [3]. To represent aluminum die casting conditions for tens of thousands of thermal cycles, the arc crucible melted samples were exposed to isothermal aging at 725 °C for 100 hours. This method avoids diffusion from the H13 base material which is unrepresentative of die casting service.

Work herein focused on metallographic preparation procedures for optical and electron microscopy needed to be developed to support microstructure characterization. Surface relief from hardness imbalances between phases complicates metallography, mandating the use of alkaline polishing media to achieve a planar surface [20]. There is a lack of research on tungsten heavy alloy—tool steel dissimilar metal clads, with only one published paper on tungsten heavy alloy—tool steel cladding. This paper did not evaluate tool steel dilution levels effect on Anviloy clad microstructure [21]. The lack of published data extends to sample preparation, especially regarding characterization of precipitates which form during thermal exposure. More information on thermal stability and precipitate formation was also required for representative die casting thermal aging conditions. This study developed sample preparation methods for tungsten heavy alloy—tool steel clads. Metallographic sample preparation methods were developed for optical microscopy, and preparation of carbon extraction replica samples were developed for TEM analysis of precipitates which form during thermal exposure. These procedures allow for microstructural characterization of all phases in tungsten heavy alloy-tool steel clads.

Methodology

A goal of this work was to develop metallographic preparation methods to improve characterization of Anviloy clad microstructure. Metallographic samples were taken from clad deposits made with hot wire gas tungsten arc welding and crucible melted controlled dilution samples. The metallographic preparation methods were used for optical microscopy, scanning electron microscopy (SEM), and transmission electron microscopy (TEM). The microstructure constituents observed were used to validate phase constituents and effects of thermal aging predicted by simulated Thermocalc phase diagrams for specific Anviloy wire – H13 dilution level fusion deposits.

Materials

Orvar supreme H13 plates that were 19 mm × 203 mm × 305 mm were provided by Uddeholm. Anviloy wire that was 1.0 mm diameter was supplied by Astaras. The composition of the H13 plates and Anviloy wire used in this study is shown in Table 1.

HW-GTAW Cladding

The HW-GTAW equipment used in this work used a Jetline 9800 mechanized system that included a, Miller Dynasty 500 and Jetline 200 Amp hot wire power supplies. Pure argon shielding gas was used for all welds using a 11,800 cc/min flow rate. HW-GTAW cladding parameters were fixed at 180 Amps, 11 Volts, 76 mm/min. travel speed, and 2032./min. wire feed speed. The hot wire used a 25 mm hot wire stick-out from the contact tip to the weld pool. Volumetric dilution was determined by measuring the cross-sectional area of base material melted into the clad fusion zone and dividing by the total clad cross-sectional area.

Arc Crucible Melting

Arc crucible melted samples were created using the system shown in Fig. 1. The system consisted of a gas tungsten arc

Table 1 Alloy compositions (wt.%)

	Fe	Cr	Mo	V	C	Si	Mn	W	Ni
H13	Bal.	5.1	1.5	0.9	0.39	0.9	0.4		
Anviloy® Wire	12.5							Bal.	27.5

Fig. 1 Arc crucible melting system

welding torch, a water cooled copper crucible, and a work chamber purged with pure argon. Samples were made with 20% H13 dilution and weighed approximately 12 grams. Orvar supreme base material was sectioned into small pieces for more uniform melting. Anviloy wire was sectioned and placed into the work chamber with orvar supreme in the desired composition and melted into flat, ovular samples.

Heat Treatment

Aging heat treatments were conducted on the arc crucible melted samples at 725 °C for 100 hours using Lucifer furnace 7GT-K24 controlled by a Honeywell DC230L controller. Isothermal aging experiments were conducted in air. Samples were water quenched following furnace removal.

Metallography

Metallography was conducted using standard metallographic grinding and polishing procedures to analyze a HW-GTAW clad and arc-crucible melted sample of the same clad composition. Samples were ground with 400, 600, and 800 grit SiC abrasive paper followed by polishing with 9, 3, and 1 micron diamond suspension. Volumetric dilution measurements were taken using standard methods [21]. ImageJ software was used to outline and measure weld reinforcement, material added, and total weld fusion zone area (weld reinforcement + melted base material. Volumetric dilution is determined by dividing weld reinforcement deposited by the total weld area. Etching procedures were developed to maximize characterization of diluted Anviloy microstructure and carbides. Samples were etched with an Alkaline Sodium Picrate solution which is known to preferentially etch M_6C carbides in tool steels [22]. Etching consisted of immersion of samples for 30–60 seconds in a solution containing 25g NaOH, 2g sodium picrate, and 100 mL water at a solution temperature of 70 °C.

Carbon Extraction Replica Method

A carbon extraction replica sample preparation method was developed to support TEM characterization. The arc-crucible melted samples were first prepared using the same polishing steps as the metallography procedure plus an additional 0.05 micron alumina step. A two stage chemical polishing procedure was developed to expose non-metal precipitates on the sample surface. The alpha BCC tungsten dendrites were planed using a 10 minute immersion in a 10% sodium hydroxide + water solution. The matrix phase was removed using a solution containing 50 mL HCL, 25 mL Phosphoric acid, 20mL Nitric Acid, and 10mL Acetic Acid and 100 mL water for 30 seconds. The final steps were used to prepare replicas. The replicas were produced using the 2 stage cellulose acetate / carbon coating procedure outlined in [23]. After carbon coating, the coated cellulose acetate tape was placed onto a TEM grid and gently exposed to 100% acetone to dissolve the tape and leave an electron transparent carbon film with embedded precipitate particles.

Scanning Electron Microscopy and Transmission Electron Microscopy

Arc crucible melted samples were analyzed using SEM and TEM. All samples were analyzed in the unetched condition using the metallography sample preparation procedure with an additional 0.05 micron alumina step. A Thermo Fisher Apreo II microscope was used for SEM imaging. The backscatter electron detector was used to promote atomic contrast between different phases.

Transmission electron microscopy (TEM) experiments were conducted on a Tecnai F20 microscope. The carbon extraction replica sample outlined above was chosen for TEM analysis. The embedded particles were imaged then analyzed using electron diffraction. A 10 micron selected area aperture was used to isolate the diffraction pattern for a single particle.

Results

Anviloy Wire—H13 HW-GTAW Clad

Figure 2 shows an unetched macro of an Anviloy wire, clad bead on plate deposit. The clad deposit was produced using hotwire gas tungsten arc welding on H13 base material as noted above. The clad deposit did not possess any weld defects such as porosity or any cracking. Good fusion to the base material was evident by the weld shape which showed adequate wetting and penetration into the base material. Volumetric dilution of H13 which was melted in the clad deposit was calculated to be approximately 20%.

Figure 3 shows a higher magnification view of the Anviloy clad deposit in the etched and unetched condition. The alkaline sodium picrate etch preferentially etched the grain boundary phase while leaving the matrix and bcc tungsten phases unetched. Note the lack of color contrast developed in the H13 based material, which contains other carbide types that were not etched by the alkaline picrate solution. A higher magnification view of the Alkaline sodium picrate etched HW-GTAW clad sample is shown in Fig. 4.

The alkaline sodium picrate solution preferentially etched the grain boundary phase in the Anviloy wire-H13 clad. No etching contrast was developed in the matrix or dendritic phases. Approximate region of Micrograph in Fig. 4 is indicated by the dashed box in Fig. 3.

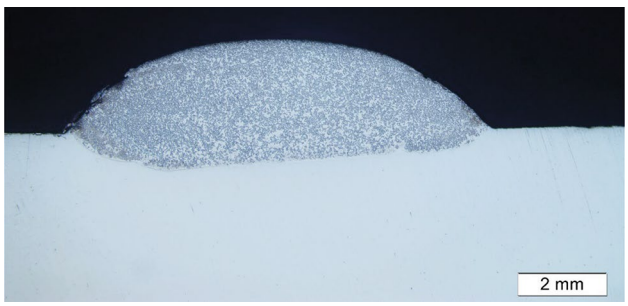

Fig. 2 Anviloy wire—H13 clad macro

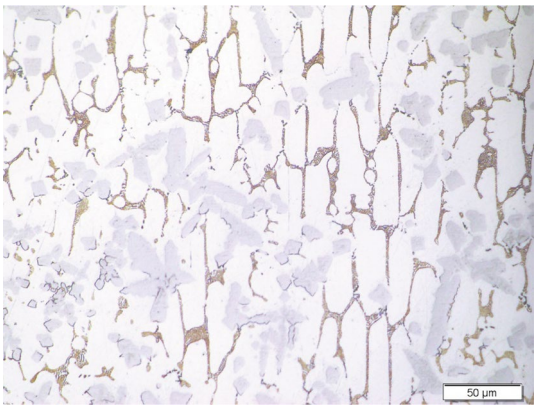

Fig. 4 Alkaline sodium picrate etched anviloy wire-H13 clad (500x)

Arc Crucible Melted Samples

Figures 5 shows the arc crucible melted sample at 2000x magnification. Figure 5 shows a structure similar to what was observed in the etched condition. A dendritic phase (Alpha BCC tungsten), matrix phase, and grain boundary phase were observed in the microstructure. Fraction of grain boundary phase was somewhat less than what was observed in HW-GTAW clads. Despite this difference, the arc-crucible melted sample microstructure appears representative of the HW-GTAW clad in that it contains the same 3 phases (Fig. 6).

After aging for 100 hours at 725 °C, the arc-crucible melted sample was etched with the alkaline sodium picrate solution. Grain boundaries appear cleanly etched in some locations, but a more diffuse contrast is developed in the aged sample versus the Anviloy wire—H13 clads. The diffuse etching along grain boundaries suggested the precipitation of fine particles preferentially along grain boundaries. Resolution was limited using optical microscopy where precipitates could not be resolved, so the aged samples were

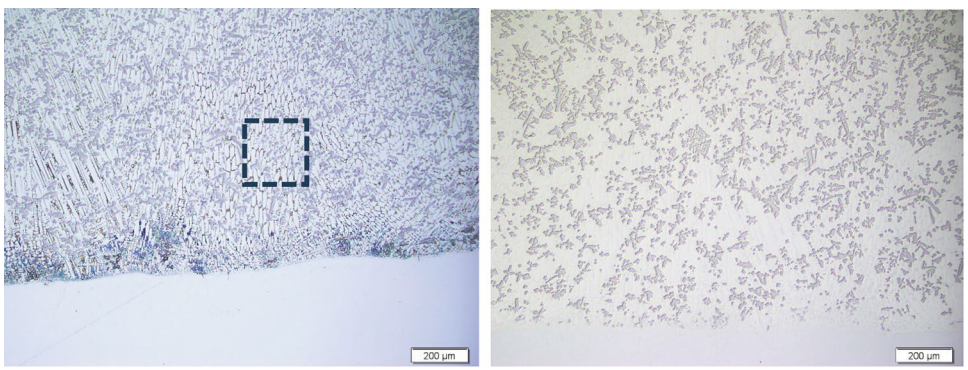

Fig. 3 Anviloy wire—H13 clad in etched (left) and unetched (right) conditions (100x)

analyzed using SEM backscatter imaging. For SEM, the aged crucible melted samples were repolished and analyzed in the unetched condition. A wide dispersion of intermetallic particles which precipitated after thermal exposure can be observed in Fig. 7. Particles appear to nucleate and form preferentially around grain boundaries, showing a similar dispersion that was observed in optical metallography using the alkaline sodium picrate etchant. Particles formed around M_6C carbides present along matrix phase grain boundaries. The presence of streaks of particles may indicate some orientation relationship with the matrix phase.

Chemical Polishing Validation

To improve microstructure definition, a sodium hydroxide treatment / chemical polish was evaluated on the arc crucible melted microstructure, Fig. 8. A pore was used to identify this specific region in the sample which was imaged before and after chemical polishing after exposure at 10 minutes to a 10% sodium hydroxide solution. The BCC alpha phase dendrites were chemical chemically polished and their surface relief was minimized. Alkaline 10% sodium hydroxide solution appeared to have minimal effect on the FCC matrix phase since no material was removed and no etching was detected. Figure 9 shows the result of the second chemical polishing procedure using a mixed acid solution, where the matrix phase was selectively dissolved without dissolution or etching of tungsten phase dendrites. These images were taken in the SEM to account for the large surface relief present after dissolving the matrix phase.

Figure 9 shows the effectiveness of the matrix chemical polishing procedure. After 60 second immersion, the true

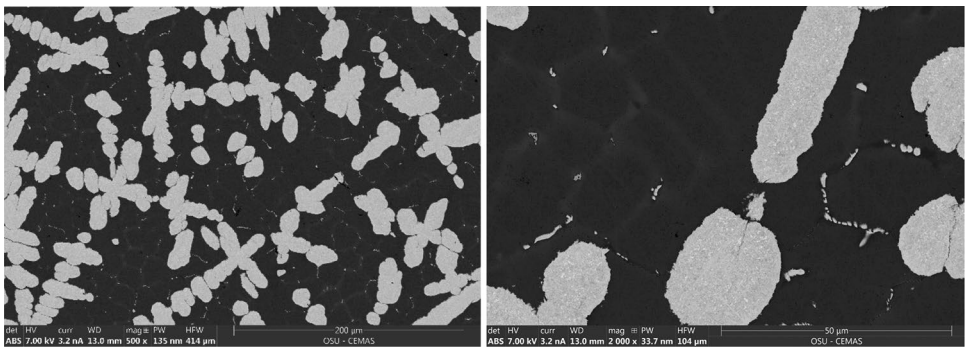

Fig. 5 As-cast arc crucible melted sample

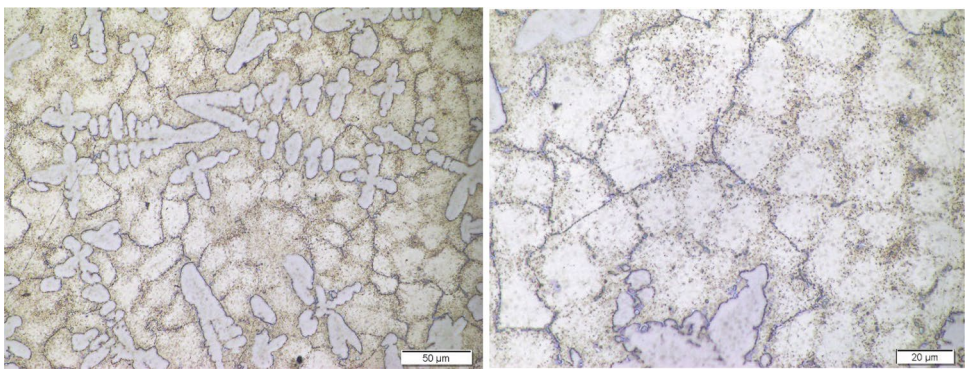

Fig. 6 Aged arc-crucible melted sample after etching with alkaline sodium picrate

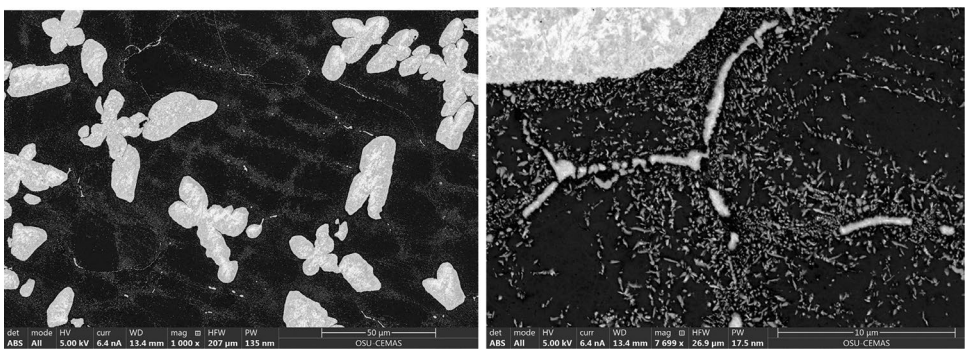

Fig. 7 Arc-crucible melted sample aged at 725 °C for 100 hours

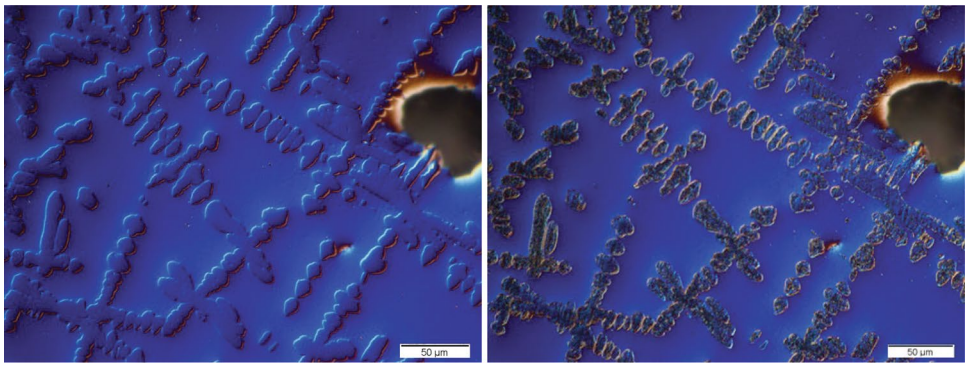

Fig. 8 Polarized light optical micrope image of aged arc crucible melted sample before (left) and after (right) 10-minute exposure in 10% aqueous NaOH

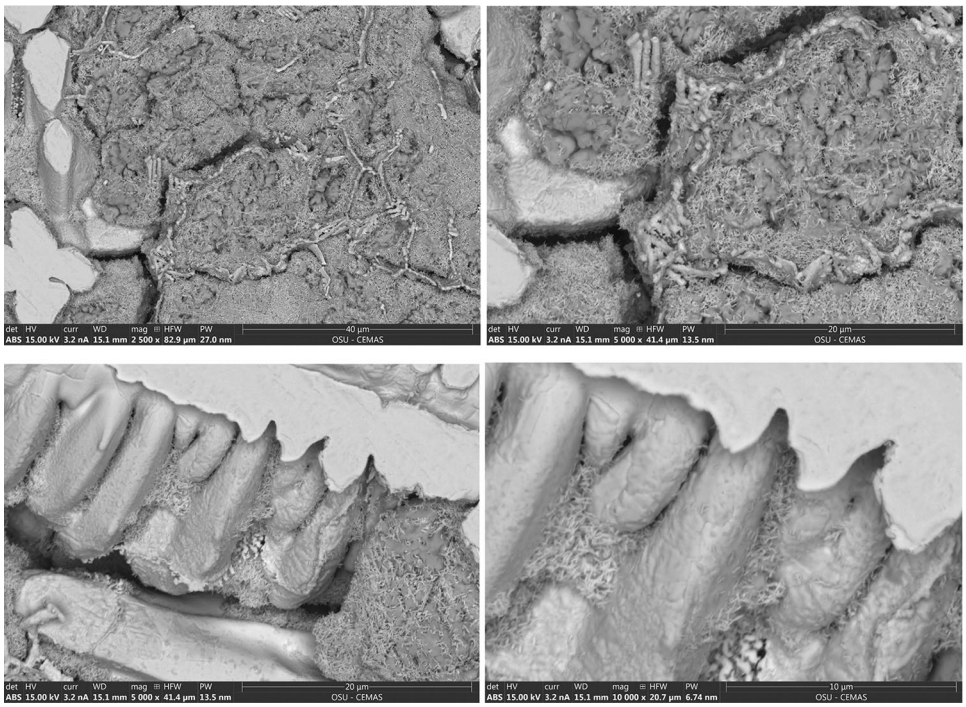

Fig. 9 SEM image of aged arc-crucible sample after 1 minute exposure to 50 mL HCL, 25 mL Phosphoric acid, 20 mL Nitric Acid, and 10 mL Acetic Acid and 100 mL Water Solution

shape of the tungsten dendrites can be observed. The presence of the flat, polished surface from mechanical grinding is still present in the tungsten dendrites shown in these images. The clean / unetched condition of these dendrites indicates the matrix polishing solution has minimal effect on the BCC tungsten phase.

A large number of intermetallic particles are still present on the sample surface after the matrix polishing procedure. The morphology of the particles appears to be unaffected by the chemical polishing procedures. Precipitates appear to be a similar size and shape as was observed in the arc Crucible cast sample that was not subjected to chemical polishing as shown in Fig. 6. These findings indicate that the two stage chemical polishing procedure exposed the precipitated particles and left them free floating on the surface of samples. To avoid excess removal of matrix phase that occurred at 60 seconds, the exposure time was reduced to 30-seconds. This chemical polishing procedure was conducted for the carbon extraction replica samples. The resulting sample which a carbon extraction replica was made from is shown in Fig. 10.

Figure 10 shows the result of the two stage chemical polishing procedure. A relatively plain surface with minimal BCC tungsten phase protrusions is observed. The matrix phase was also successfully removed, resulting in a high number of intermetallic particles present on the sample surface. Since the matrix phase was dissolved around these particles, they are essentially free floating in the sample surface and can be removed using the carbon extraction replica method. A TEM image of the carbon extraction replica sample is shown in Fig. 11.

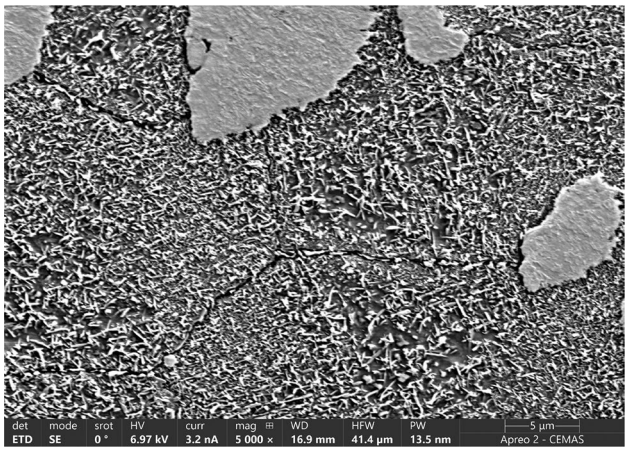

Fig. 10 SEM image aged arc-crucible melted sample after two step chemical polishing procedure

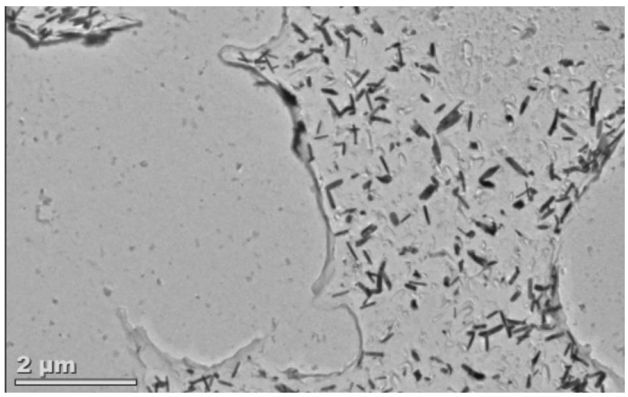

Fig. 11 TEM image of carbon extraction replica sample

TEM Analysis

Figure 11 shows precipitate particles embedded in the carbon film with a similar morphology to what was observed in the SEM study of bulk samples. Both morphology and orientation of precipitate particles appears to be maintained in the carbon extraction replica. The replica method appears to show the outline of prior BCC tungsten grain locations. A higher magnification image of a precipitate is shown in Fig. 12 along with a diffraction pattern obtained from the particle.

The higher magnification of the precipitate shown in Fig. 12 shows some evidence of faulting indicated by the arrow. The diffraction pattern shown in Fig. 12 is consistent with that gathered for the mu phase intermetallic particle. Acquisition of high quality imaging and diffraction data indicated the developed carbon extraction method was effective at characterizing the precipitates which formed after thermal exposure of the crucible melted dilution sample.

Discussion

Metallographic analysis of the Anviloy wire—H13 clad shown in Figs. 2 and 3 confirmed standard polishing procedures were effective. In the unetched condition, the BCC tungsten phase and FCC matrix phase show good natural color contrast, making analysis of these phases relatively simple. Regarding the grain boundary M_6C phase, color contrast is somewhat intermediate between matrix and BCC phases which complicated analysis. Etching was required to improve characterization and evaluation of the grain boundary phase. Previous work on tungsten heavy alloy—tool steel clads did not discuss metallographic etchants or characterization of third phase particles. Previous work on tool steels

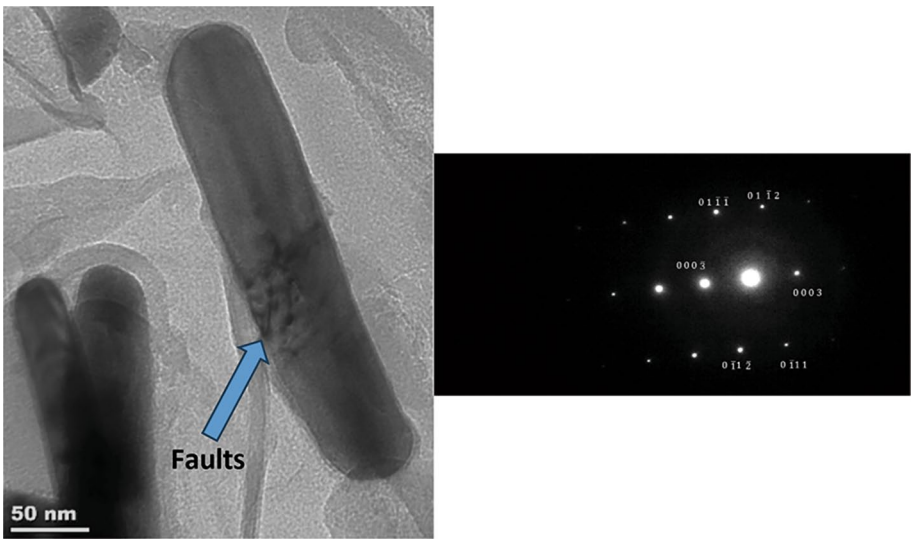

Fig. 12 TEM image showing stacking faults in particles (left) and electron diffraction pattern from a particle (right)

indicated that some solutions, namely alkaline sodium picrate, preferentially etch carbides with high periodic group VI refractory metal content, but this work did not evaluate similar materials [22].

The alkaline sodium picrate solution etch method allowed for more effective analysis of the grain boundary phase in the HW-GTAW clad due to the improved color contrast. The etchant was effective at darkening the grain boundary phase, revealing a skeletal morphology that was not evident in the unetched condition. Contrast developed from the alkaline sodium picrate etch here suggests that, although developed for tool steel grades, this solution may be effective at identifying M_6C carbide phase in a wider range of alloy compositions such as tungsten heavy alloy clads. This work confirms the BCC and FCC phases of the tungsten heavy alloy clad microstructure were not attacked by the alkaline sodium picrate etch. Interestingly, some grains of BCC tungsten phase, particularly ones close to the fusion boundary, etched along their edges. This could indicate the formation of an M_6C carbide phase at the interface between BCC tungsten and FCC phases. Further characterization will be required to confirm presence of interfacial M_6C carbides outlining BCC tungsten phase.

Optical metallographic analysis of the arc crucible melted sample aged 100 hours at 725 °C was not able to resolve any microstructural change in the unetched condition. After exposure to the alkaline sodium picrate etch, the aged arc-crucible melted sample developed contrast along matrix phase grain boundaries. Contrast along grain boundaries in this sample was more diffuse versus the M_6C phase seen in the HW-GTAW clad, where sharp color contrast neatly defined the matrix phase grain boundaries coated with M_6C carbide. The different appearance in the two conditions suggested some microstructural evolution occurred after thermal exposure and that the alkaline sodium picrate solution preferentially etched the precipitated phase. It is likely that whichever phase precipitated during thermal exposure was not large enough to resolve in optical microscopy, resulting in the diffuse etching appearance.

SEM analysis of the aged arc crucible melted sample confirmed the presence of a fine precipitate which formed during thermal exposure. A somewhat diffuse precipitation of this phase along grain boundaries was observed in the SEM, similar to what was observed in metallography using the alkaline picrate etch. Diffuse precipitation can be identified in the unetched condition in the SEM due to high atomic number contrast between the precipitated phase and matrix / BCC tungsten phase. The precipitated phase was on the order of hundreds of nanometers in size, which explains why it was difficult to resolve using metallography due to optical microscopes' limited resolution. Despite their small individual size, etching with alkaline sodium picrate appears able to resolve precipitate clusters. Alkaline sodium picrate solution likely etched these precipitates or their interface with the surrounding material due to their high tungsten content.

Previous work on tungsten heavy alloy—tool steel clads did not evaluate effect of dilution. These previous studies did not discuss precipitate of carbide or intermetallic phases which may form in clads. Methods for evaluating fine precipitates are required to better understand aging phenomena in this material combination. This work developed a method for extraction replica analysis of precipitates to facilitate direct observation. Work began by developing a two-step chemical polishing method which dissolves matrix and BCC tungsten phases without affecting precipitates. Validation of the two step chemical polishing procedure was necessary since this method has not previously been published. It is widely known that strongly alkaline solutions such as sodium hydroxide can be used to chemically polish tungsten. For Anviloy diluted clad deposits, a new polishing procedure was needed to improve phase identification. Since the tungsten phase is harder / more wear resistant than the matrix phase in tungsten heavy alloys, mechanical polishing with conventional abrasives results in surface relief where the BCC tungsten grain protrude slightly from the matrix. Protrusion of tungsten grains and non-planar surfaces complicates microscopic analysis. In particular, nanohardness, EDS, or EBSD data gathered on a non-flat surface may have significant error. Protrusions also complicate extraction replica sample preparation. Therefore, it was beneficial to have a method for flattening samples after mechanical polishing. Previous work mandated the use of strong alkaline solutions during polishing, which can be present a chemical hazard to workers [24]. Using the method developed herein, samples can be chemically polished to acceptable flatness in fume hoods after polishing, lessening the risk of chemical exposure.

The use of polarized light in the optical microscope helped resolve the effect of sodium hydroxide solution on tungsten phase dimensional offset, clearly showing chemical polishing after a 10 minute exposure. The matrix phase appeared unaffected by the sodium hydroxide treatment, possibly due to its corrosion resistance in alkaline environments. FCC matrix phases in tungsten heavy alloys are known to contain high tungsten contents if cooled quickly from solidification, up to 9 at.% [25]. Molybdenum and Tungsten are in the same periodic group and have similar effect when used as alloying elements in nickel based alloys, primarily increasing localized and alkaline corrosion resistance [26, 27]. Because of this high tungsten concentration, matrix phase in tungsten heavy alloys likely has similar properties to Hastelloy B type nickel based alloys with high Molybdenum contents. This could explain the resistance of the tungsten heavy alloy matrix phase to alkaline solutions such as the 10% sodium hydroxide solution used to chemically polish tungsten grains.

The second chemical polishing step was confirmed to have little effect on the BCC tungsten, M_6C carbide, and intermetallic precipitates which supported its use as a chemical polishing agent for tungsten heavy alloys. All of these phases were observed after the matrix chemical polishing step in similar morphologies as before etching. Use of this solution for 60 seconds exposed large portions of Tungsten grains, giving insight to their true shape and morphology. The presence of detached intermetallic particles was also evident. Because the particles of interest for TEM analysis were essentially free floating on surfaces after chemical polishing, it was important to conduct all chemical polishing with sample surface facing upwards. This condition used gravity to ensure loose particles remained on the surface until they could be extracted.

Carbon coating and sample extraction using cellulose acetate tape resulted in successful acquisition of images and diffraction patterns of fine particles from the arc-crucible melted sample. This confirmed the effectiveness of the two step procedure for analysis of tungsten heavy alloy precipitates. The method developed herein allowed for characterization of fine precipitates that form in tungsten heavy alloy clads. Since many intermetallic particles have complex crystal structures, navigating to a crystal zone axis can be more complicated than cubic crystal structures. Navigating to a zone axis is especially difficult when there is a background matrix component in diffraction patterns, as is the case in FIB foil extractions which contain intermetallic precipitates still embedded in their matrix phase. For mu phase intermetallic, there are several orientation relations possible with the FCC matrix phase as well as some reports of incoherent precipitation [28, 29]. The use of carbon extraction replica sample preparation allows for analysis of particles of interest alone by separating them from the matrix phase. Extraction simplifies analysis of particles smaller than TEM apertures, which is sometimes difficult in FIB foil analysis.

Conclusions

This work details the metallographic preparation methods that were developed for microstructure characterization of Anviloy clad deposits and arc melted diluted cast samples on H13 tool steel. The cast samples were evaluated in the as-cast and aged conditions where the latter used a heat treatment representative of die cast die peak temperature exposure. As-clad microstructure contained BCC tungsten and FCC phase as well as M_6C carbide which was resolved using an alkaline sodium picrate etchant. The alkaline sodium picrate etchant produced color contrast in the M_6C carbide phase which formed on solidification during cladding. Etchant contrast was also developed by alkaline sodium picrate solution in the aged arc-crucible melted samples. Though their small size prevented direct observation of individual intermetallic particles in optical microscopy, the color contrast developed around intermetallic clusters indicated alkaline sodium picrate solution preferentially etched mu phase particles. SEM analysis of aged arc-crucible melted samples confirmed the etching contrast developed in optical microscopy was due to mu phase intermetallic clusters. SEM imaging showed similar dispersion preferentially along matrix phase grain boundaries as observed in optical microscopy.

The two step chemical polishing procedure was validated using optical microscopy and SEM analysis. The 10% aqueous sodium hydroxide solution was shown to preferentially remove the BCC tungsten dendrites without attacking the matrix phase or intermetallic particles after 10 minutes. Likewise, the 30 second mixed acid chemical polishing step was shown to remove the matrix phase without affecting BCC tungsten phase or intermetallic particles. These two chemical polishing steps produced a microscopically flat sample surface enabling extraction of loose intermetallic particles on the sample surface via cellulose acetate tape. Carbon coating of the cellulose acetate and subsequent dissolution of the tape in acetone resulted in an electron transparent carbon film with embedded intermetallic particles. TEM analysis of the extraction replica sample confirmed the intermetallic that formed after aging was mu phase.

References

1. A. Endemann, T. Hoehn, New materials in mould making are required to meet the new challenges in die casting. Paper presented at the 73rd World Foundry Congress "Creative Foundry, WFC 2018 - Proceedings, 489–490 (2018)
2. N. Senthilnathan, A. Raja Annamalai, G. Venkatachalam, Sintering of tungsten and tungsten heavy alloys of W-Ni–Fe and W–Ni–Cu: a review. Trans. Indian Inst. Met. (2017). https://doi.org/10.1007/s12666-016-0936-2
3. D. Schwam, J. Wallce, S. Birceanu, Die materials for critical applications and increased production rates. Case Western Reserve University (2002)
4. Y. Şahin, Recent progress in processing of tungsten heavy alloys. J. Powder Technol. (2014)
5. R.M. German, A. Bose, S.S. Mani, Sintering time and atmosphere influences on the microstructure and mechanical properties of tungsten heavy alloys. Metall. Trans. A. **23**, 211–219 (1992)

6. G.V. Raynor, V.G. Rivlin, Critical evaluation of constitutions of certain ternary alloys containing iron, tungsten, and a third metal. Int. Metals Rev. **26**(1), 213–240 (2013)
7. E. Semenova, MIST., Fe-Ni-W ternary phase diagram evaluation., MSI Eureka (2014)
8. F.R. Winslow, The iron-nickel-tungsten phase diagram, U.S. At. Energy Comm. Pubn, Phase Diagram, Phase Relations, Review, Y-1758 (1971)
9. J. Das, G. Appa Rao, S.K. Pabi, Microstructure and mechanical properties of tungsten heavy alloys. Mater. Sci. Eng. A. **527**(29–30), 7841–7847 (2010)
10. D.V. Edmonds, P.N. Jones, Interfacial embrittlement in liquid-phase sintered tungsten heavy alloys. Metall. Trans. A. **10A**, 289–295 (1979)
11. J.M. Walsh, M.J. Donachie, On a new intermetallic phase in the nickel-tungsten system. Metall. Trans. A. **4**(12), 2854–2855 (1973).
12. A.M. Zakharov, V.G. Parshikov, L.S. Vodop'yanova, V.A. Novozhonova, Phase equilibria in alloys of the W-Fe-CoNi system. I. Alloys containing 10% (Fe+Co+Ni) at 1400–1200°C. Sov. Powder Metall. Met. Ceram. **4**, 313–316 (1986)
13. A.V. Nikol'skii, A.M. Zakharov, V.G. Parshikov, L.S. Vodop'yanova, Phase equilibria in the tungsten-rich field of the W-Fe-Ni system in the 800–575°C. Sov. Powder Metall. Met. Ceram. **8**, 675–680 (1991)
14. R. Cury, J.-M. Joubert, S. Tusseau-Nenez, E. Leroy, A. Allavena-Valette, On the existence and the crystal structure of Ni4W, NiW and NiW2 compounds. Intermetallics. **17**(3), 174–178 (2009)
15. H.H. Stadelmaier, C. Suchjakul, Overview of the quaternary system iron-nickel-tungsten-carbon. Int. J. Mater. Res. **76**(3), 157–161 (1985)
16. C. Yin, D. Terentyev, T. Zhang, S. Nogami, S. Antusch, C.-C. Chang, R.H. Petrov, T. Pardoen, Ductile to brittle transition temperature of advanced tungsten alloys for nuclear fusion applications deduced by miniaturized three-point bending tests. Int. J. Refract Metal Hard Mater. (2021). https://doi.org/10.1016/j.ijrmhm.2020.105464
17. V. Krsjak, S.H. Wei, S. Antusch, Y. Dai, Mechanical properties of tungsten in the transition temperature range. J. Nucl. Mater. (2014). https://doi.org/10.1016/j.jnucmat.2013.11.019
18. A.J. Clayton, Application for anviloy 1150 in aluminum and brass die casting. Precis. Metals. **30**(7), 29–31 (1972)
19. J. L. Kovacich, *Anviloy Wire - H13 Cladding Development*, Master's thesis, Available from Ohio State University, Thesis completed December, 2020.
20. A. Skumavc, J. Tušek, A. Nagode, L. Kosec, Tungsten heavy alloy as a filler metal for repair welding of dies for high pressure die casting. Int. J. Mater. Res. (2013). https://doi.org/10.3139/146.110963
21. J. Lippold, *Welding Metallurgy and Weldability* (Wiley, Hoboken, New Jersey, 2015)
22. G. Vander Voort, Metallographic Preparation of Tool Steels, Beuhler Tech Notes 5(3) (2015)
23. M. Rolinska, F. Gustavsson, P. Hedström, Revisiting the applications of the extraction replica sample preparation technique for analysis of precipitates in engineering alloys. Mater. Charact. (2022). https://doi.org/10.1016/j.matchar.2022.111978
24. Z. Jiao, R. Kang, Z. Dong, J. Guo, Microstructure characterization of W-Ni-Fe heavy alloys with optimized metallographic preparation method. Int. J. Refract. Metal Hard Mater. (2019). https://doi.org/10.1016/j.ijrmhm.2019.01.011
25. G.V. Raynor, V.G. Rivlin, Critical evaluation of constitutions of certain ternary alloys containing iron, tungsten, and a third metal. Int. Metals Rev. **26**(1), 213–249 (1981)
26. A.P. Brown, The corrosion behavior of molybdenum and hastelloy B in sulfur and sodium polysulfides at 623 K. J. Electrochem. Soc. **134**(8), 1921–1925 (1987)
27. M. Obradović, J. Stevanović, A. Despić, R. Stevanović, J. Stoch, Characterization and corrosion properties of electrodeposited Ni-W alloys. J. Serbian Chem. Soc. **66**(11–12), 899–912 (2001)
28. M. Pessah-Simonetti, P. Caron, P. Donnadieu, T. C. P. phase particles embedded in a superalloy matrix: Interpretation and prediction of the orientation relationships. [Topologically close packed]. United States. doi.org/https://doi.org/10.1016/0956-716X(94)90307-7
29. C.-M. Lin, W.-Y. Kai, Su. Cherng-Yuh, K.-H. Key, Empirical alloys-by-design theory calculations to the microstructure evolution mechanical properties of Mo-doped laser cladding NiAl composite coatings on medium carbon steel substrates. J. Alloy. Compd. (2017). https://doi.org/10.1016/j.jallcom.2017.01.278